BMB
Reports

Biochemical characterization of ferredoxin-NADP$^+$ reductase interaction with flavodoxin in *Pseudomonas putida*

*Jinki Yeom & Woojun Park**

Department of Environmental Science and Ecological Engineering, Korea University, Seoul 136-713, Korea

Flavodoxin (Fld) has been demonstrated to bind to ferredoxin-NADP$^+$ reductase A (FprA) in *Pseudomonas putida*. Two residues (Phe^{256}, Lys^{259}) of FprA are likely to be important for interacting with Fld based on homology modeling. Site-directed mutagenesis and pH-dependent enzyme kinetics were performed to further examine the role of these residues. The catalytic efficiencies of FprA-Ala^{259} and FprA-Asp^{259} proteins were two-fold lower than those of the wild-type FprA. Homology modeling also strongly suggested that these two residues are important for electron transfer. Thermodynamic properties such as entropy, enthalpy, and heat capacity changes of FprA-Ala^{259} and FprA-Asp^{259} were examined by isothermal titration calorimetry. We demonstrated, for the first time, that Phe^{256} and Lys^{259} are critical residues for the interaction between FprA and Fld. Van der Waals interactions and hydrogen bonding were also more important than ionic interactions for forming the FprA-Fld complex. [BMB Reports 2012; 45(8): 476-481]

INTRODUCTION

Ferredoxin-NADP$^+$ reductases (Fprs; EC 1.18.1.2) are ubiquitous, monomeric, reversible flavin enzymes. They have a prosthetic flavin cofactor (FAD) and catalyze the reversible electron exchange between NADPH and ferredoxin (Fd) or flavodoxin (Fld) (1). Generally, Fpr interacts with Fd in the electron transfer process. Some bacteria and algae possess a Fld, which has a flavin mononucleotide (FMN) cofactor. Fld is a highly acidic protein that can substitute for Fd as the electron carrier under iron-depleted conditions. Fld can also act as a substitute for Fd by accepting electrons from Fpr in various metabolic processes, such as photosynthesis, nitrogen fixation, biotin synthesis, and nitric oxide synthesis (2).

The crystal structures of several plant-type Fpr proteins consist of two domains (3, 4). The first N-terminal domain is composed of a scaffold of six antiparallel strands arranged in two perpendicular β-sheets that bind to FAD. The second domain (C-terminal) contains an NADP(H) binding site within a core of five parallel β-strands surrounded by seven α-helices (1, 4). Fd binds to a concave surface of the FAD binding region of the Fpr and transfers electrons (3, 4). The hydrophobic condition generates entropic changes, which give rise to the transfer of electrons between the electron donor and acceptor. Thus, catalytic activity is generated in the hydrophobic region near the FAD-binding site (3). This Fpr cleft region interacts with both Fd and Fld, despite their structural differences (5).

The catalytic activity (k_{cat}) of the typical plastid-type Fprs is much higher (200～500 s^{-1}) than that of the bacterial Fprs (0.4～1 s^{-1}) (1). Bacterial Fprs can be further categorized into two subclasses (1). In subclass I Fpr, the key C-terminal residue is phenylalanine, whereas in subclass II the phenylalanine is replaced by tryptophan (1). These residues interact with the adenine moiety of the FAD. Bacteria typically have one *fpr* gene in their chromosome. However, some proteobacteria, including *Pseudomonas putida,* possess two annotated *fpr* genes (*fprA* and *fprB*) (6, 7). Bacterial subclasses I and II have different metabolic functions (1).

P. putida has just one Fld-encoding gene, whose homolog is annotated as *mioC* in *E. coli*, and this gene encodes an electron carrier for biotin synthesis (8). The role of the Fld (*mioC*) in *P. putida* has not been determined (3, 9). Due to the number of different physiological roles for both Fd and Fld, electron exchange between Fpr and either Fd or Fld can be a very important cellular process in prokaryotic cells. We have reported that Fprs in *P. putida* function as ferredoxin/flavodoxin reductase and determined their preferred redox partner (10). The catalytic efficiency of FprA is higher when Fld is present as its redox partner when compared to the kinetics observed with other electron transport partners. In particular, the Fpr forms a specific complex with [3Fe-4S] Fd through ionic interactions formed between the Lys residues of Fpr and Asp/Glu residues of [3Fe-4S] Fd in *Azotobacter vinelandii* (11). However, the role of the Fpr Lys residue in the interaction between Fpr and [2Fe-2S] Fd/Fld has not yet been examined. Additionally, the binding thermodynamics of bacterial Fprs with their partners

*Corresponding author. Tel: +82-2-3290-3067; Fax: +82-2-953-0737;
E-mail: wpark@korea.ac.kr
http://dx.doi.org/10.5483/BMBRep.2012.45.8.071

**Received 23 March 2012, Revised 2 May 2012,
Accepted 21 May 2012**

Keywords: Ferredoxin-NADP$^+$ reductase, Flavodoxin, Isothermal titration calorimetry, Protein-protein interaction, *Pseudomonas putida* KT2440

have not yet been systematically evaluated. Therefore, in this study, we examined the function of the Lys residue of the *P. putida* Fpr using isothermal calorimetry (ITC).

The enzyme kinetics of wild-type Fprs and site-directed mutants were characterized to elucidate the *P. putida* Fpr binding mechanism. Furthermore, we examined, for the first time, the thermodynamic parameters of bacterial Fprs and their redox partners. Our data show that the lysine residue is important for the association between FprA and Fld. In addition, FprA had a larger positive change in enthalpy (ΔH) with Fld, which indicated that van der Waals interactions and hydrogen bonding were more important than ionic interactions.

RESULTS

Identification of the crucial residue in the interaction between Fprs and their redox partners

We have previously identified the preferred redox partners of two Fprs (FprA and FprB) (10). The highest specific constant (k_{cat}/K_m) of FprA and FprB was observed in the presence of Fld and FdA, respectively. The pH-dependent enzyme kinetics were characterized to determine the electron transfer mechanism between Fprs and substrates, and all data were processed using a Dixon plot (Fig. 1A) (12). The pK_a of the ionizable groups of essential active site residues involved in the catalysis were determined by plotting pH versus the k_{cat} values. Then, 0 slope (on the top of bell shaped curve of the bottom graph in Fig. 1) absolute maximum slope lines were drawn on the left and right sides. The intersection points of absolute maximum slope lines on the 0 slope line represented pK_{a1} and pK_{a2}, respectively (12). Interestingly, the most important residues during the reaction in the case of complex formation between FprA and Fld were histidine and lysine, because of their pK_a values (6.0 and 10.5, respectively) (Fig. 1A). However, the histidine and tyrosine residues were important for their interaction in the case of the FprB-FdA complex, as the pK_a values of these residues were 6.0 and 10.1, respectively (Fig. 1B). Histidine is an essential residue for electron transfer in Fpr (13). However, the function of other resides, such as tyrosine and lysine, during the interaction have not yet been examined using kinetic and thermodynamic tools. Additionally, the residues crucial to the electron transfer properties and thermodynamics of bacterial Fpr have not been identified.

Kinetics of FprA and Fld binding using site-directed mutagenesis

The kinetic properties of *P. putida* Fprs with their redox partners have been examined using a cytochrome *c* reduction assay (13). The Fd-dependent NAD(P)H cytochrome c reductase assay shows that FprB strongly prefers FdA (10). When Fld was used as an electron acceptor in the cytochrome *c* reduction assay, it strongly interacted with FprA, with a very low K^{Fld}_m value (10). FprA has a high catalytic efficiency (k^{FprA}_{cat}/K^{Fld}_m) when paired with Fld, indicating that Fld is the preferred redox partner of FprA (10).

The bacterial Fpr subclass I is represented by *A. vinelandii* Fpr, and their functions are modulated by phenylalanine residues (1, 11). Therefore, we performed site-directed mutagenesis of the phenylalanine residue in the *P. putida* FprA C-terminal region (FprA-Phe^{256}). Interestingly, the k_{cat} value of FprA-Phe^{256} was 8-fold lower than that of the wild-type FprA with Fld (Table S1). Thus, the catalytic efficiency (k_{cat}/K_m) was 8-fold lower than that of the wild-type FprA. However, the K_m value of FprA-Phe^{256} did not change. Therefore, the phenylalanine residues in the FprA C-terminal region may be important for transferring electrons to Fld, but the phenylalanine residues did not affect binding affinity (K_m) between FprA and Fld. Subsequently, we performed site-directed mutagenesis of the FprA C-terminal lysine residue (FprA-Lys^{259}). The lysine residue has a positively charged side chain at pH 7.4, and the

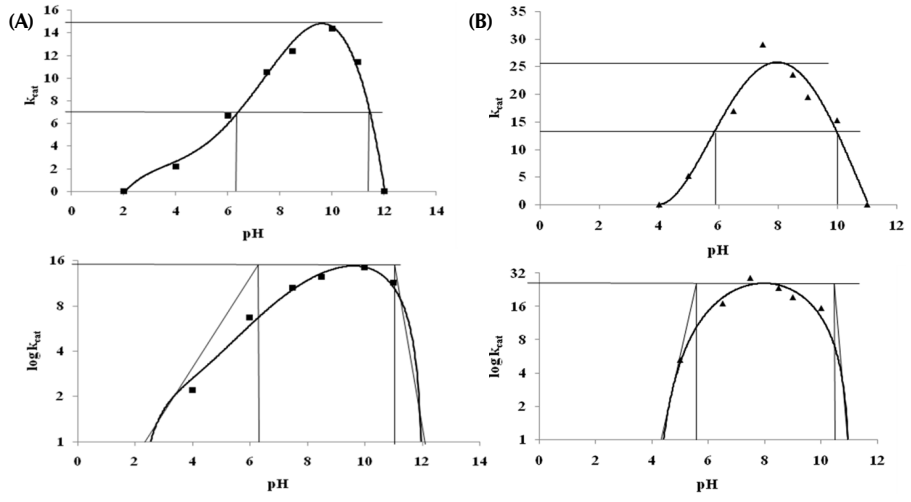

Fig. 1. Enzyme kinetics of ferredoxin-NADP$^+$ reductases (Fprs) depend on pH. The cytochrome *c* assay, which depends on pH, was performed to predict the active site. The upper figure shows the raw kinetic data for the combination between (A) FprA and flavodoxin (Fld) and (B) FprB and FdA. The lower figure was graphed using a Dixon plot to calculate the pKa values.

positive residue is important for the interaction between Fpr and its substrate (1, 11). Therefore, we constructed two site-directed mutants, an alanine substituted and an aspartic acid substituted, and these mutants had a different amino acid charge at neutral pH (FprA-Ala^{259} and FprA-Asp^{259}). The polarities and charge properties of alanine and aspartic acid are different from those of lysine. The k_{cat} values of FprA-Asp^{259} and FprA-Ala^{259} were 3.09 $e^{-}s^{-1}$ and 3.62 $e^{-}s^{-1}$, respectively, which were smaller than that of wild type (6.34 $e^{-}s^{-1}$). The K_m value of FprA-Ala^{259} increased slightly, but the K_m value of FprA-Asp^{259} was similar to that of the wild type. Thus, the catalytic efficiencies (k_{cat}/K_m) of two-site directed mutant proteins were 2-fold lower than those of the wild-type FprA with Fld. Our data demonstrate that both the phenylalanine and lysine residues of the FprA C-terminal region were important for electron transfer to Fld.

Homology modeling of wild-type and site-directed mutated FprA with Fld

Based on the structure of the Fpr complex in maize leaves (14), the distance between FAD of Fpr and the iron-sulfur center of Fd was about 6.0 Å. We previously used docking-model predictions and found that the distances between the FAD and FMN cofactors in various FprA-Fld complexes is approximately 9.79 Å (10), indicating that the two molecules may interact and exchange electrons via cofactors. The phenylalanine residue (red color in Fig. 2) was adjacent to the FAD cofactor in the FprA model. Phenylalanine is important for proper functioning of bacterial subclass I Fpr, such as FprA (1). Our previous data showed that FprA has many basic residues (Arg48, Arg52, Lys94, Lys95 and Arg245) near the Fld docking location (10). Fld, which is more acidic than Fd, may be stabilized by the basicity of the Arg and Lys residues during their interaction (1). To investigate the function of Lys^{259} in *P. putida* FprA, the binding model structures was predicted using homology modeling and a docking prediction program (Fig. 2). In the wild-type FprA, the Lys^{259} residue was located close to the FAD cofactor (2.8 and 3.8 Å) (Fig. 2A). Lys^{258} of *A. vinelandii* Fpr has hydrogen bonds with FAD phosphate oxygens (11). Lys^{258} also makes van der Waals contacts to the ribose of FAD. Therefore, our data indicate that the Lys^{259} residue of FprA may form a salt bridge with the FAD cofactor in *P. putida*. In particular, FprA may form a salt bridge with the FAD cofactor in *P. putida* considering the distance of 2.8 Å between the amino group of Lys^{259} and the FAD cofactor (Fig. 2A). Although the distance between the backbone part of each amino acid residue and FAD cofactor was 3.8 Å, the functional groups of FprA-Ala^{259} and FprA-Asp^{259} were not located near the FAD cofactor (Fig. 2B and C). Therefore, electron transfer of FprA-Ala^{259} and FprA-Asp^{259} proteins may be difficult, because of the large distance between the amino acid residue and the FAD cofactor of the FprA-Ala^{259} and FprA-Asp^{259} proteins.

Thermodynamic relationship between Fprs and partners

ITC was used to study the thermodynamic catalytic reaction of Fpr (Fig. 3), and the thermodynamic parameters of the interaction between Fpr and substrate are summarized in Supplementary Table S2. The observed change in enthalpy, ΔH_{obs}, was calculated from the true binding enthalpy change, ΔH_{bind}, and the buffer enthalpy change, ΔH_{buff}, according to:

$$(1)\ \Delta H_{obs} = \Delta H_{bind} + n_{H+} + \Delta H_{buff}$$

where n_{H+} is the number of protons released from the Tris buffer at a specific temperature (293K), previously calculated as a single proton in the Fpr/Fd reaction in the buffer (15). The heat capacity change (enthalpy change depending on temperature change), ΔCp, was also calculated according to the ITC parameters. The change in nonpolar and polar solvent-accessible surface areas was then calculated as follows:

$$(2)\ \Delta Cp_{bind} = 0.45\Delta A_{np} - 0.26\Delta A_p$$
$$(3)\ \Delta H_{bind} = -8.44\Delta A_{np} + 31.4\Delta A_p$$

where ΔCp_{bind} and ΔH_{bind} are represented by cal mol^{-1} K^{-1} and cal mol^{-1}, respectively. The calculated ΔA_{np} and ΔA_p are displayed as $Å^2$.

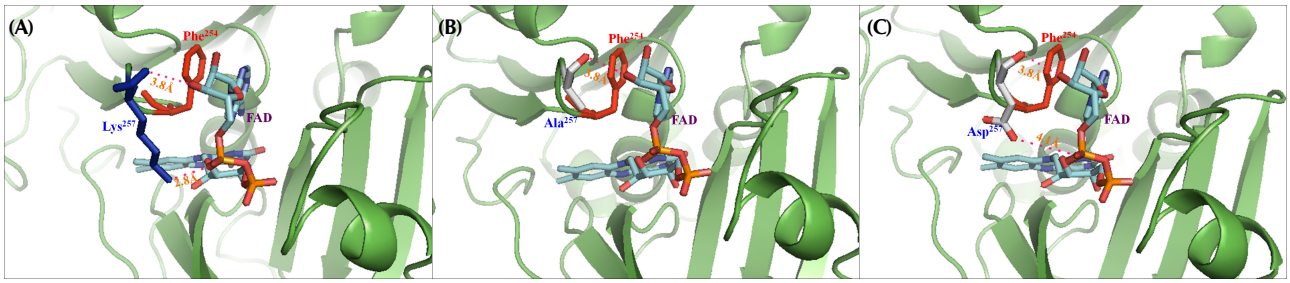

Fig. 2. Homology protein model of the ferredoxin-NADP$^+$ reductase A (FprA) with the prosthetic flavin cofactor (FAD). FprA is shown in green. (A) The complex of the FprA and FAD cofactor is displayed with the FprA active site. The lysine and phenylalanine resides near the active site are shown in blue and red, respectively. The FprA-Ala^{259} (B) and FprA-Asp^{259} (C) with FAD are displayed with the active site.

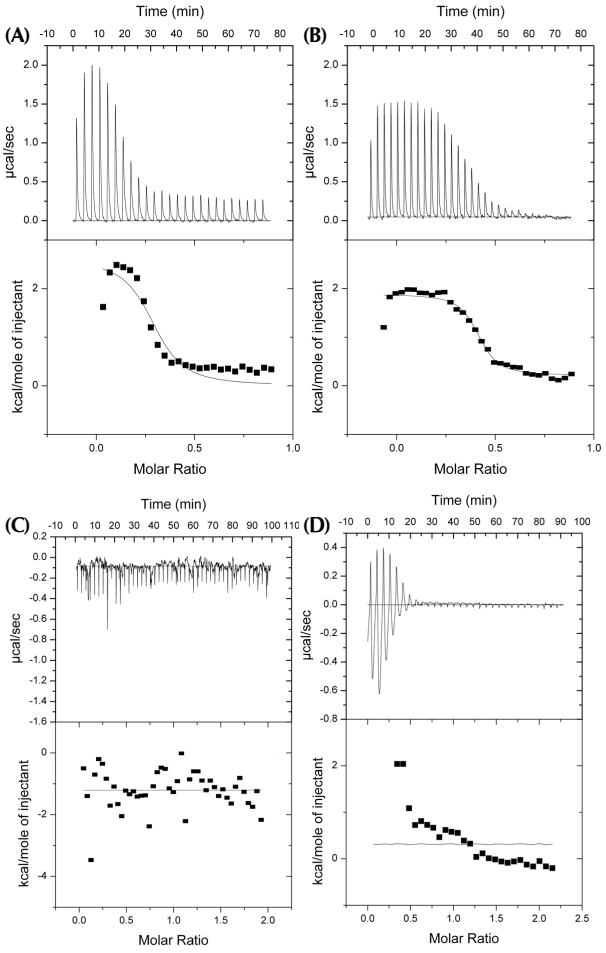

Fig. 3. Experimental calorimetric titrations from the characterization of the binary complexes formed between ferredoxin-NADP$^+$ reductase (Fpr) and their substrates. Titration of FprA (0.5 mM in the calorimetric cell) with flavodoxin (Fld) (20 mM in the syringe) in Tris-Cl (50 mM; pH 7.8) (A); FprB (0.5 mM) with Fd (20 mM) in Tris-Cl (50 mM; pH 7.8) (B); FprA-Ala^{259} (0.5 mM) with Fld (20 mM) in Tris-Cl (50 mM; pH 7.8) (C); FprA-Asp^{259} (0.5 mM) with Fld (20 mM) in Tris-Cl (50 mM; pH 7.8) (D) at 293K.

The entropy change (ΔS) is described as

$$(4)\ \Delta S = \Delta S_{hydro} + \Delta S_{vib}$$
$$(5)\ \Delta S_{hydro} = 1.35\Delta Cp_{bind}\ln(T/386)$$

where ΔS_{hydro} is the contribution of the hydrophobic effect and ΔS_{vib} represents the contribution of intramolecular vibration in the binding reaction (16).

The interaction between Fpr and Fd usually slightly increases ΔH and has a large positive contribution to $T\Delta S$ (15, 16). In the case of FprA and Fld, FprA produced a larger positive change in ΔH, and had a smaller positive contribution to $T\Delta S$ than the typical plastid Fpr reaction (Fig. 3A and Table S2) (15, 16). Although

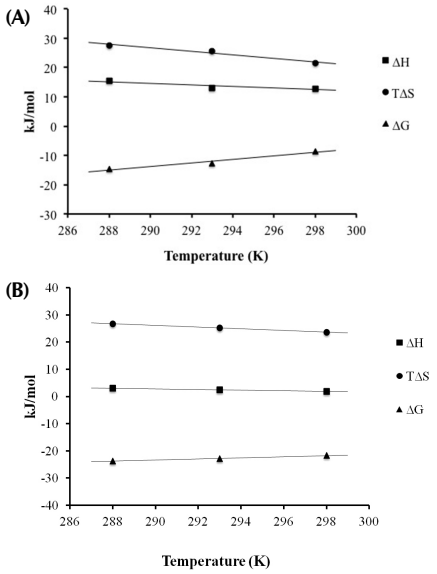

Fig. 4. Dependence of the measured enthalpy of the binary complex formation on temperature for ferredoxin-NADP$^+$ reductase A (FprA)/flavodoxin (Fld) (A) and FprB/ferredoxin (Fd) (B). The Gibbs free energy (ΔG), heat of binding change (ΔH), and entropy change (ΔS) were calculated according to materials and methods equation.

the interaction between FprA and Fld resulted in a more positive change in ΔH than reported previously, the compensation of Gibbs free energy was influenced by $T\Delta S$. The enthalpy of binding (ΔH_{bind}) was calculated using Equation 1, and, accordingly, the calculated change in heat capacity (ΔCp_{bind}), which is equivalent to the slope, was -62.11 cal mol^{-1} K^{-1}. Linear regression analysis of the measured ΔH_{bind} at different temperatures (Fig. 4A and Table S2) yielded a ΔCp_{bind} of -0.26 kJ mol^{-1} K^{-1}. Subsequently, ΔA_{np} and ΔA_p were calculated to be -248.44 and 191.11 Å^2, respectively, using Equations 2 and 3 (Table S2). These results indicate that the hydrophobic effect was a major contributor to binding. The positive entropy change ($T\Delta S$) under the various temperature conditions indicated that the binding reaction was driven by a very strong hydrophobic effect. As shown in Equations 4 and 5, ΔS_{hydro} was calculated from ΔCp_{bind}, and ΔS_{hydro} and ΔS_{vib} were calculated to be 96.76 and -9.05 J mol^{-1} K^{-1}, respectively (Table S2). Because the Gibbs free energy was influenced by the entropy (ΔS) of the association with FprA and Fld, ΔS_{hydro} was stronger than ΔS_{vib}, indicating that the interaction between FprA and Fld might be driven by the hydrophobic effect.

In the case of a combination FprB and FdA, the parameters important to this complex were more similar to those of *Anabaena* Fpr (15) than those of the complex between FprA and Fld. The parameters of this interaction had a similar positive entropy ($T\Delta S$) and less positive enthalpy (ΔH_{bind}) than the FprA/Fld complex; thus, this interaction was driven primarily by changes in entropy (Fig. 4B and Table S2). The complex between FprB and

FdA also had a negative heat capacity change (ΔCp_{bind}) and more nonpolar surface area (ΔA_{np}) than polar surface area, and the entropy change was driven by the hydrophobic effect (ΔS_{hydro}) in this reaction (Fig. 4B and Table S2).

Interestingly, it seems likely that site-directed mutant FprA-Ala^{259} and FprA-Asp^{259} proteins did not interact with the Fld substrate in the ITC test (Fig. 3C and D). In particular, FprA- Ala^{259} did not bind to the Fld substrate in the ITC experiment (Fig. 3C). In fact, the raw data pattern of FprA-Ala^{259} was similar to the ITC data obtained for the control buffer (data not shown). However, it seemed likely that FprA-Asp^{259} bound slightly to Fld (Fig. 3D). Although the raw FprA-Asp^{259} data contained several peaks, these data were not properly calculated. Therefore, site-directed mutant FprA-Ala^{259} and FprA-Asp^{259} proteins may not transfer electrons to Fld, and these binding events may not have changed the thermodynamic properties of the protein.

DISCUSSION

In all bacterial Fprs, an aromatic residue is found in the position occupied by the carboxyl terminal tyrosine in the plastidic Fpr (1). This residue interacts with the adenine moiety of FAD. A completely conserved tryptophan fulfills this role in bacterial subclass II, which is replaced by a phenylalanine in subclass I (1). However, other residues surrounding the FAD binding site of Fpr have not been characterized. The lysine of *A. vinelandii* might play a role in the interaction with FAD through the formation of a salt bridge, although its function has not been confirmed (11). The enzyme kinetic data in the present study suggested that Phe^{256}, which is important for binding to Fld (1), and Lys^{259} was the crucial residue for electron transfer with Fld. (Table S1). Interactions between the positive residues on the Fpr surface and acidic residues on Fd generally contribute to protein-protein recognition (1, 17). However, the K_m value of the FprA-Ala^{259} and FprA-Asp^{259} proteins did not change, and their thermodynamic parameters could not be calculated with Fld, suggesting that Lys^{259} may influence the interaction with FAD, not through electrostatic interaction, but rather through direct electron transfer, which changed the k_{cat} value (Table S1). Several studies have suggested that lysine residues are important for stabilizing the FAD cofactor (18) and the amino group of the lysine residue near the FAD cofactor could facilitate electron transfer from FAD to the substrate (18).

Fprs of *P. putida* had a larger ΔH_{bind} value than reported previously, suggesting that van der Waals interactions and hydrogen bonding are more important than ionic interactions (Table S2). Ionic interactions through acidic and basic residues are essential for the interaction between Fpr, plastid type, and Fd, [2Fe-2S] type (1, 17). However, putidaredoxin, [2Fe-2S] ferreodoxin type, and putidaredoxin reductase are driven more by van der Waals forces and hydrogen bonding than ionic interactions (16). The interactions between FprA and FprB have a negative ΔC_p value, which is consistent with our results in which a strong hydrophobic effect was observed for the association between Fpr and its redox partners. Both Fd and Fld can play similar roles by interacting with the same partners, despite having a different molecular size, topology, and redox cofactors (1). In addition, replacement of negatively charged or hydrophobic side chains on the Fld surface had no effect on binding, indicating that these side chains are not involved in specific interactions (17). Therefore, the interaction between Fpr and Fld appears to be less specific than that with Fd. Also, Fld bound to a smaller region in Fpr; thus, its residues are less critical for binding. In this study, the lower ΔC_p value for Fld binding also suggested that the interaction interface in the FprA and Fld complex was smaller than that in the FprB and Fd complex (Table S2). Interestingly, the energetics of apoFld binding to Fpr was not related to that of Fld in *Anabaena* (17), suggesting that Fpr interacts with apoFld and Fld through different binding modes. Determining the direct role of the FMN molecule in the interaction of Fld with Fpr will be important to understand the mechanism of the interaction between FprA and Fld.

MATERIALS AND METHODS

Bacterial strains, plasmids, and growth conditions

Bacterial strains, plasmids, primers, and bacterial growth conditions have been described previously (10).

Protein purification

All purification steps were performed at 4°C using an fast protein liquid chromatography (FPLC) system (AKTA FPLC, Amersham Bioscience, Piscataway, NJ, USA). The methods used for protein purification were described previously (10).

Site-directed mutagenesis

Site-directed mutants were constructed via a three step-four primer overlap/extension polymerase chain reaction (PCR) technique, using Platinum Pfx (Invitrogen, Carlsbad, CA, USA) (19-21). The first step was prepared via PCR amplification with the primer pairs FprA F/SDM AR (CCCGCCTGCGCCTTACGC CTCGACGAAGGCACG) and FprAR/SDMAF (CGTGCCTTCGT CGAGGCGTAAGGCGCAGGCGGG) (alanine mutant) or FprAF/SDMDR (CCCGCCTGCGCCTTAGTCCTCGACGAAGG CACG) and FprAR/SDMDF (CGTGCCTTCGTCGAGGACTAA GGCGCAGGCGGG) (aspartic acid mutant) or FprAF/SDMFR (GCCTTACTTCTCGACGGCGGCAC GTTCGATCAG) and FprAR/ SDMFF (CTGATCGAACGTGCCG CCGTCGAGAAGTAAGGC) (phenylalanine mutant). Each of the PCR products was annealed at the region overlap and extended to form full-length double-strand mutant DNA. The full-length mutant DNA was amplified using primers for FprAF/FprAR.

Homology modeling of the protein complex

The methods used for homology model generation and the docking model were described previously (10).

Enzyme kinetics for analysis of catalytic activity

The methods used for enzyme kinetics were described previously (10).

Analysis of protein interactions using ITC

All ITC experiments were performed using an Omega titration calorimeter (MicroCal). Experiments were performed in Tris-Cl (50 mM; pH 7.8) and temperatures were maintained between 15 and 25°C throughout the measurements. Fpr and Fld were extensively purified by dialysis in the same buffer to ensure that the ITC results were accurate. The reaction cell contained 1.4 ml of FprA or FprB solution with 0.25 mM NADPH in the same buffer. The injection syringe was filled with FdA or Fld, and the solutions were stirred at 351 rpm during titration. The titration was conducted by performing 20 injections of 5 μl of the substrate solution, with the injections spaced by 420 seconds. Gibbs free energy (ΔG) was calculated using the following equation to accurately account for the contribution of entropy to binding:

$$\Delta G = \Delta H\text{-}T\Delta S \text{ and } \Delta G = \text{-}RT\ln K$$

where R is the gas constant, and T is the absolute temperature. The parameters determined by ITC were K, dissociation constant; ΔH, heat of binding change; and ΔS, entropy change (15, 16).

Acknowledgements

This work was supported by the MEST/NRF program (grant #: 2011-0002711) to W.P.

REFERENCES

1. Ceccarelli, E. A., Arakaki, A. K., Cortez, N. and Carrillo, N. (2004) Functional plasticity and catalytic efficiency in plant and bacterial ferredoxin-NADP(H) reductases. *Biochim. Biophys. Acta*. **1698**, 155-165.
2. Sancho, J. (2006) Flavodoxins: sequence, folding, binding, function and beyond. *Cell Mol. Life Sci*. **63**, 855-864.
3. Kurisu, G., Kusunoki, M., Katoh, E., Yamazaki, T. and Teshima, K. (2001) Structure of the electron transfer complex between ferredoxin and ferredoxin-NADP(+) reductase. *Nat. Struct. Biol*. **8**, 117-121.
4. Sridhar-Prasad, G., Kresge, N., Muhlberg, A. B., Shaw, A., Jung, Y. S. and Burgess, B. K. (1998) The crystal structure of NADPH: ferredoxin reductase from *Azotobacter vinelandii*. *Protein Sci*. **7**, 2541-2549.
5. Martinez-Julvez, M., Medina, M. and Gomez-Moreno, C. (1999) Ferredoxin-NADP(+) reductase uses the same site for the interaction with ferredoxin and flavodoxin. *J. Biol. Inorg. Chem*. **4**, 568-578.
6. Lee, Y., Peña-Llopis, S., Kang, Y. S., Shin, H. D., Demple, B., Madsen, E. L., Jeon, C. O. and Park, W. (2006) Expression analysis of the *fpr* (ferredoxin-NADP+ reductase) gene in *Pseudomonas putida* KT2440. *Biochem. Biophys. Res. Commum*. **339**, 1246-1254.
7. Lee, Y., Yeom, J., Kang, Y. S., Kim, J., Sung, J. S., Jeon, C. O. and Park, W. (2007) Molecular characterization of *fprB* (ferredoxin-NADP+ reductase) in *Pseudomonas putida* KT2440. *J. Microbiol. Biotechnol*. **17**, 1504-1512.
8. Birch, O. M., Hewitson, K. S., Fuhrmann, M., Burgdorf, K., Baldwin, J.E., Roach, P.L. and Shaw, N. M. (2000) MioC is an FMN-binding protein that is essential for *Escherichia coli* biotin synthase activity *in vitro*. *J. Biol. Chem*. **275**, 32277-32280.
9. Hu, Y., Li, Y., Zhang, X., Guo, X., Xia, B. and Jin, C. (2006) Solution structures and backbone dynamics of a flavodoxin MioC from *Escherichia coli* in both Apo- and Holo-forms: implications for cofactor binding and electron transfer. *J. Biol. Chem*. **281**, 35454-35466.
10. Yeom, J., Jeon, C. O., Madsen, E. L. and Park, W. (2009) *In vitro* and *in vivo* interactions of ferredoxin-NADP$^+$ reductases in *Pseudomonas putida*. *J. Biochem*. **145**, 481-491.
11. Jung, Y.S., Roberts, V. A., Stout, C. D. and Burgess, B. K. (1999) Complex formation between *Azotobacter vinelandii* ferredoxin I and its physiological electron donor NADPH-ferredoxin reductase. *J. Biol. Chem*. **274**, 2978-2987.
12. Riaz, M., Rashid, M. H., Sawyer, L., Akhtar, S., Javed, M. R., Nadeem, H. and Wear, M. (2012) Physiochemical properties and kinetics of glucoamylase produced from deoxy-D-glucose resistant mutant of *Aspergillus niger* for soluble starch hydrolysis. *Food Chem*. **130**, 24-30.
13. Fischer, F., Raimondi, D., Aliverti, A. and Zanetti, G. (2002) *Mycobacterium tuberculosis* FprA, a novel bacterial NADPH-ferredoxin reductase. *Eur. J. Biochem*. **269**, 3005-3013.
14. Kurisu, G., Kusunoki, M., Katoh, E., Yamazaki, T. and Teshima, K. (2001) Structure of the electron transfer complex between ferredoxin and ferredoxin-NADP(+) reductase. *Nat. Struct. Biol*. **8**, 117-121.
15. Jelesarov, I. and Bosshard, H. R. (1994) Thermodynamics of ferredoxin binding to ferredoxin: NADP$^+$ reductase and the role of water at the complex interface. *Biochemistry* **33**, 13321-13328.
16. Aoki, M., Ishimori, K., Fukada, H., Takahashi, K. and Morishima, I. (1998) Isothermal titration calorimetric studies on the associations of putidaredoxin to NADH-putidaredoxin reductase and P450cam. *Biochim. Biophys. Acta*. **1384**, 180-188.
17. Martínez-Júlvez, M., Medina, M. and Velázquez-Campoy, A. (2009) Binding thermodynamics of ferredoxin: NADP$^+$ reductase: two different protein substrates and one energetic. *Biophys. J*. **96**, 4966-4975.
18. Hellerman, L. and Coffey, D. S. (1967) Studies on crystalline D-amino acid oxidase. V. Characterization of borohydride-reduced enzyme-substrate intermediate. Synthesis of epsilon-N-(1-carboxyethyl)-L-lysine. *J. Biol. Chem*. **242**, 582-589.
19. Ho, S. N., Hunt, H. D., Horton, R. M., Pullen, J. K. and Pease, L.R. (1989) Site-directed mutagenesis by overlap extension using the polymerase chain reaction. *Gene* **77**, 51-59.
20. Asghari, S. M., Khageh, K., Dalfard, A. B., Pazhang, M. and Karbalaei-Heidari, H. R. (2011) Temperature, organic solvent and pH stabil: zation of the neutral protease from saling vibrio nrotedyticus: significance of the strutural calcium. *BMB Rep*. **44**, 665-668.
21. Zhang, R., Cui, Y., Zhang, X., Yang, Z., Zhao, Y., Song, Y., Wu, C. and Zhang, J. (2010) Soluble expression, purtication and the role of C-terminal glycine residues in scorpion toxin BmK AGP-SYPU2. *BMB Rep*. **43**, 801-806.